Optics Letters

Ramsey interferometry of a bosonic Josephson junction in an optical cavity

SHENG-CHANG LI,[1,*] FU-QUAN DOU,[2] AND LI-BIN FU[3,4]

[1]School of Science, Xi'an Jiaotong University, Xi'an 710049, China
[2]College of Physics and Electronic Engineering, Northwest Normal University, Lanzhou 730070, China
[3]Graduate School, China Academy of Engineering Physics, Beijing 100193, China
[4]Center for Applied Physics and Technology, Peking University, Beijing 100084, China
*Corresponding author: scli@xjtu.edu.cn

Received 4 July 2017; revised 4 September 2017; accepted 5 September 2017; posted 7 September 2017 (Doc. ID 301357); published 27 September 2017

We investigate the nonlinear Ramsey interferometry of a bosonic Josephson junction coupled to an optical cavity by applying two identical pumping field pulses separated by a holding field in the time domain. When the holding field is absent, we show that the atomic Ramsey fringes are sensitive to both the cavity-pump detuning and the initial state, and their periods can encode the information on both the atom-field coupling and the atom-atom interaction. For a weak holding field, we find that the fringes characterized by the oscillation of the intra-cavity photon number can completely reflect the frequency information of the atomic interference due to the weak atom-cavity coupling. This finding allows a nondestructive observation of the atomic Ramsey fringes via the cavity transmission spectra.

OCIS codes: (020.1475) Bose-Einstein condensates; (120.3180) Interferometry; (130.4310) Nonlinear.

https://doi.org/10.1364/OL.42.003952

The Ramsey interferometry [1] is equivalent to the famous double-slit interference in the time domain, which forms a cornerstone of the interferometry in both optics and quantum mechanics. Indeed, the collisional interaction in dilute ultracold gases plays an important role in both the dynamics of Bose-Einstein condensates (BECs) and the formation of molecules [2]. Based on the Ramsey interferometry method, the *s*-wave scattering lengths in a two-component BEC [3] have been measured, and a magnetic tensor gradiometer by interferometrically measuring the relative phase between two spatially separated BECs has been realized [4]. In particular, taking advantage of the pairwise scattering interaction in a BEC, a two-mode BEC of N atoms has been used to implement a nonlinear Ramsey interferometer [5] whose detection uncertainty scales better than the optimal $1/N$ Heisenberg scaling of linear interferometry [6].

In ultracold atomic gases, the nonlinearity stems from atom-atom interactions, treated by mean-field approximation (MFA). Such interactions cause an effect such as self-trapping of the atoms in a double-well (DW) potential [7]. The system of a BEC in a DW potential is a good candidate for realizing analogs of a bosonic Josephson junction (BJJ) [8]. Recently, the great achievements in manipulating ultracold atoms in an optical cavity open a new avenue of studying the dynamics in quantum many-body systems [9]. Moreover, there have been great advances in controlling and probing the cold atoms in both an optical lattice [10] and an optical lattice in a cavity [11–13]. The strong atom-cavity coupling has been realized in experiment by using an atomic BEC [14,15]. An ultracold atomic ensemble interacting with the high-finesse cavity modes is a typical system of cavity quantum electrodynamics that provides an ideal platform for exploring exotic many-body quantum effects [16–23], which has witnessed a significant development [24,25] in both quantum optics and cold atom physics.

In this Letter, to precisely measure the BJJ in an optical cavity, we construct a nonlinear Ramsey interferometer by applying a sequence of two identical pumping field pulses to a system that consists of an atomic BEC trapped in a DW potential. Both wells are coupled to a single-mode optical cavity with frequency ω_c, which is pumped by an external coherent field at frequency ω_p (see Fig. 1). We consider the dispersive-interaction regime where the pump is weak and the detuning is large and, thus, the excited state of the atoms can be adiabatically eliminated. We employ the theoretical model given in Ref. [26], which was based on both two-mode approximation [27] and MFA. The dynamics of the system is governed by the equations

$$\frac{dz}{dt} = -\sqrt{1-z^2}\,\sin\phi, \tag{1}$$

$$\frac{d\phi}{dt} = rz + \frac{z}{\sqrt{1-z^2}}\cos\phi + \frac{\delta U_0}{2\Omega}|\alpha(z,t)|^2, \tag{2}$$

where the dimensionless variables z and ϕ denote the atomic population imbalance and the relative phase between the two traps, respectively. The dimensionless parameter $r \equiv NU/(2\Omega) > 0$ measures the interaction strength (U denotes the repulsive interaction strength between a pair of atoms in

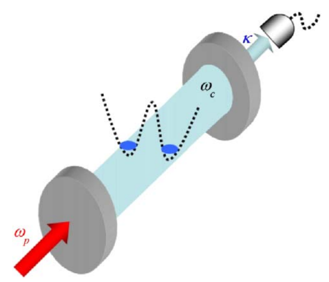

Fig. 1. Schematic of the system. A DW potential loaded with ultracold atoms is coupled to an optical cavity that accommodated two wells. The cavity is pumped by an external coherent field, and the signal leaking out of the cavity is measured to infer the key features of the atomic system.

the same trap) against the tunneling strength (Ω is the tunneling matrix element between the two atomic modes) with N being the total number of atoms. The time has been rescaled in units of the Rabi oscillation time $1/(2\Omega)$, i.e., $2\Omega t \to t$. The dimensionless parameter δ reflects the coupling difference between the two atomic modes and the cavity mode [28]. The parameter U_0 represents the effective atom-photon coupling strength at an antinode. The average photon number,

$$|\alpha(z,t)|^2 = \frac{A(t)^2}{(z-B)^2 + C^2}, \tag{3}$$

implies that the cavity field always follows the dynamics of the condensate adiabatically [29]. The parameters $A(t) = \eta(t)/(\delta U_0 N/2)$ ($\eta(t)$ is the pumping field strength), $B = \Delta/(\delta U_0 N/2)$ (Δ denotes the cavity-pump detuning), and $C = \kappa/(\delta U_0 N/2)$ (κ is the cavity-leakage rate) can be understand as the reduced pumping strength, reduced detuning, and reduced loss rate, respectively. The MFA allows us to study the dynamics in the Josephson regime [30], which is characterized by $1/N \ll U/\Omega \ll N$.

Note that the variables z and ϕ form a pair of conjugate variables, and the corresponding Hamiltonian $H = H(z,\phi;t)$ can be written as

$$H = \frac{1}{2}rz^2 - \sqrt{1-z^2}\cos\phi + \frac{\tilde{A}(t)}{C}\arctan\left(\frac{z-B}{C}\right), \tag{4}$$

where $\tilde{A}(t) = \delta U_0 A^2(t)/(2\Omega)$. It should be mentioned that the first two terms in Eq. (4) are the energy of a bare BJJ [7], and the last term describes a cavity-field-induced asymmetry of the BJJ. In this Letter, we assume that the pumping strength $\eta(t)$ varies in time and, thus, the Hamiltonian is explicitly time-dependent. For convenience, we adapt a two-pulse Ramsey scheme

$$\tilde{A}(t) = \begin{cases} \tilde{A}_h + \tilde{A}_0 \sin^2(\omega t), & 0 \le t \le T, \\ \tilde{A}_h, & T < t < t_1, t > t_2, \\ \tilde{A}_h + \tilde{A}_0 \sin^2[\omega(t-t_1)], & t_1 \le t \le t_2, \end{cases} \tag{5}$$

with $t_1 = T + t_h$ and $t_2 = 2T + t_h$. In this scheme, there are two identical pumping field pulses of the length $T = \pi/\omega$, with a holding time of t_h between them. In our weak coupling case, the strength of the holding field $\tilde{A}_h$ is very small, i.e., $\tilde{A}_h \ll \tilde{A}_0$.

To begin our numerical experiments, initially, we prepare the system in the state $(z(t=0), \phi(t=0)) = (z_0, \phi_0)$, and then evolve it for a time duration t_2; finally, we measure the atomic population imbalance between the two traps, i.e., $z(t_2)$, which is our effective output. Varying the holding time t_h and repeating the above procedure, we can obtain the two-pulse Ramsey fringes in the time domain. In this Letter, we set the parameters as [26] $\tilde{A}_0 = 0.02$, $\omega = 0.5$, $C = 0.07$, and $r = 3$. With the help of the fourth–fifth order Runge–Kutta algorithm with an adaptive step, we solve the coupled Eqs. (1) and (2). For different detuning Δ and initial states with $\tilde{A}_h = 0$, we obtain the Ramsey fringes characterized by the oscillation of $z(t_2)$ with t_h (in units of $1/(2\Omega)$), as shown in Fig. 2. The main features of the exotic Ramsey fringes demonstrated in Fig. 2 include (1) most of the fringes are different from the standard Ramsey fringes of sinusoidal or cosinoidal form; (2) the period of the atomic fringes is very sensitive to the initial state; and (3) the visibility of the fringes is non-zero which is a link to the tunneling parameter between the two wells. In addition, we see that the visibility strongly depends on the initial state for the cases $z_0 \simeq \pm 1$ [see Figs. 2(a) and 2(c)]; the visibility is much lower than that for the case $z_0 = \pm 0.5$ [see Figs. 2(b) and 2(d)].

In contrast to both the shape and the visibility of the fringes, the period of the fringes is more crucial in practice. For example, in the experiment for measuring the binding energy of the molecular state in BEC, it turned out that the period of the fringes is accurately determined by the Feshbach molecular energy in the holding time [31]. Subsequently, we make a theoretical analysis on the period properties of the fringes, illustrated in Fig. 2. For a given detuning, we extract the period of the fringes by employing the fast Fourier transformation (FFT) technique. For each initial state, we apply the FFT to six fringes (with different Δ) and demonstrate the corresponding periods (marked by solid squares) in Fig. 3.

Now we understand the above exotic numerical results through some analytical deduction. To this end, we need to know the role of the first pumping pulse played in the dynamical evolution. In our calculations, $T = \pi/\omega = 2\pi$ is of the same order of the intrinsic timescale for the atomic tunneling, i.e., $2\pi/\Omega = 4\pi$. With the emergence of the

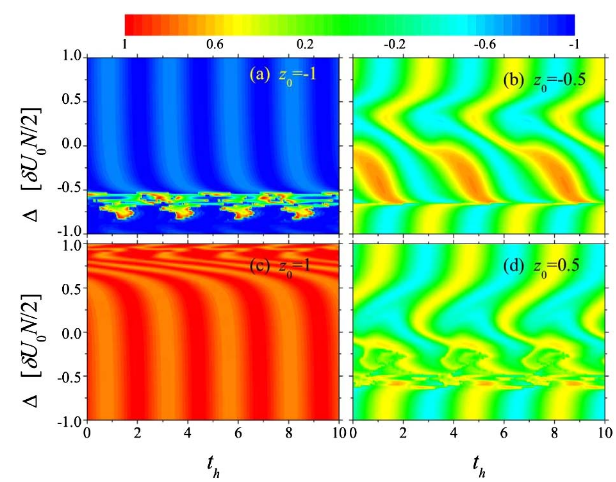

Fig. 2. Atomic Ramsey fringes in the time domain for different initial states. (a) $(z_0, \phi_0) \simeq (-1, 0)$, (b) $(z_0, \phi_0) = (-0.5, 0)$, (c) $(z_0, \phi_0) \simeq (1, 0)$, and (d) $(z_0, \phi_0) = (0.5, 0)$. The degree of color indicates $z(t_2)$. The parameters are $\tilde{A}_0 = 0.02$, $\tilde{A}_h = 0$, $\omega = 0.5$, $C = 0.07$, and $r = 3$.

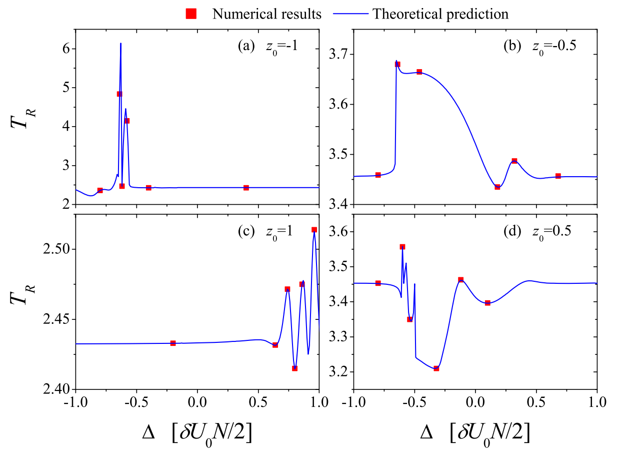

Fig. 3. Periods of the Ramsey fringes as a function of the detuning Δ (in units of $\delta U_0 N/2$) for different initial states. (a) $(z_0, \phi_0) \simeq (-1, 0)$, (b) $(z_0, \phi_0) = (-0.5, 0)$, (c) $(z_0, \phi_0) \simeq (1, 0)$, and (d) $(z_0, \phi_0) = (0.5, 0)$. The solid lines show our theoretical prediction given by Eq. (6), and the scatter squares denote the numerical results obtained from the FFT analysis.

atom-cavity-field coupling, from the standpoint of the atoms, the coupling makes the DW potential asymmetric and further modifies the atomic tunneling dynamics. Seen by the cavity field, the atoms have distinct back-action on the light field, i.e., the coupling can shift the cavity resonance frequency and, hence, can modify the field intensity [see Eq. (3)]. For the general case, including both the atom-atom interaction and the atom-field coupling, the time-dependent system (4) is no longer analytically solvable. Our simulations with different initial states and various detuning parameters for the atomic population imbalance $z(T)$ and the energy of the system $H(T)$ (when the first pumping pulse turns off) are displayed in Figs. 4(a) and 4(b), respectively. We find that both the initial state and the detuning can affect the dynamics and the energy of the system significantly.

Compared with the dynamics during the first-pulse duration, the dynamics during the holding time becomes simple due to the uncoupling (i.e., $\tilde{A}_h = 0$) of the cavity field from

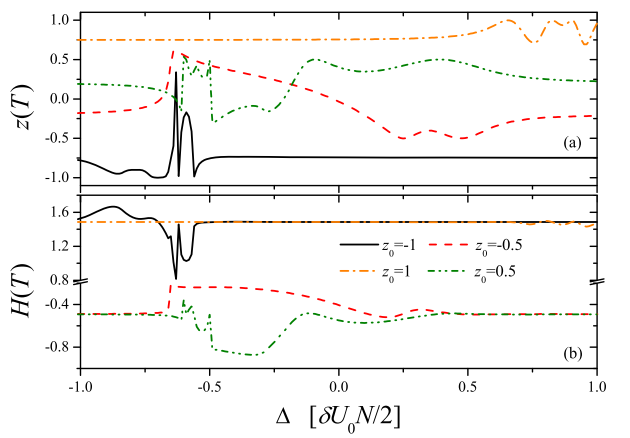

Fig. 4. (a) Atomic population imbalance $z(T)$ and (b) classical energy of the system $H(T)$ as a function of the detuning Δ (in units of $\delta U_0 N/2$) for different initial states. The same parameters are used as in Fig. 2.

the BJJ. When $t \in [T, t_1]$, the system is autonomous and the Hamiltonian is conserved. The trajectory of the system in the phase space (plane) follows the manifold (line) of constant energy. Thus, qualitatively speaking, the dynamics of the system is to a great extent determined by the structure of trajectory. The trajectories of the BJJ are often periodic orbits with cyclic lines in the phase space. This type of motion is the so-called Rabi oscillation (the oscillation of z) of the BJJ. The period of the Rabi oscillation can be evaluated by taking advantage of the conservation of the energy (4) (during the time t_h) whose value is $H(T)$, which is

$$T_R = \oint \left| \frac{\partial \phi}{\partial H} \right| \mathrm{d}z = 2 \int_{z_{\min}}^{z_{\max}} F(z) \mathrm{d}z, \tag{6}$$

with

$$F(z) = \left[\sqrt{1 - z^2} \sqrt{1 - \frac{[rz^2 - 2H(T)]^2}{4(1 - z^2)}} \right]^{-1}, \tag{7}$$

where $z_{\max}$ and $z_{\min}$ correspond to the maximum and the minimum of the reachable atomic population imbalance $z(t)$ during the holding time, respectively. They are determined by $\frac{r^2}{4} z^4 + [1 - rH(T)] z^2 + H(T)^2 - 1 = 0$. When $H(T) \in [-1, 1]$, we have $z^{\pm} = \pm G^{+}(z)$ with $G^{\pm}(z) = \frac{\sqrt{2}}{r}[H(T)r - 1 \pm \sqrt{1 - 2H(T)r + r^2}]^{1/2}$, and $(z_{\max}, z_{\min}) = (z^{+}, z^{-})$. When $H(T) \in [1, \frac{1+r^2}{2r}]$, we get $z_1^{\pm} = \pm G^{+}(z)$, $z_2^{\pm} = \pm G^{-}(z)$, and $(z_{\max}, z_{\min}) = (\max[z_1^-, z_2^-], \min[z_1^-, z_2^-])$ or $(\max[z_1^+, z_2^+], \min[z_1^+, z_2^+])$. Equation (6) is our main result in this Letter. The periods calculated from this equation are demonstrated in Fig. 3, which are in good agreement with the numerical results based on the FFT analysis.

A simple physical understanding of this perfect consistence can be given in terms of the Rabi orbits in the phase space. As mentioned before, during the holding time, the energy (4) is time-independent and, thus, we can view the system as a closed system. For a given initial state, the system evolves with time following a periodic motion and constructs a cycle trajectory in the phase space. This closed Rabi orbit is often an ellipse or a circle, which is equivalent with the motion of a one-dimensional harmonic oscillator. For this closed system, the energy is preserved, i.e., $H(t) = H(T) =$ constant when $t \in [T, t_1]$. The period of this cycle motion is determined by $T_R = 2\pi/\omega_R = 2\pi I/H(T)$, where ω_R is the corresponding frequency of the Rabi oscillation; the action $2\pi I$ equals the phase-space area enclosed by the closed orbit. To see the connection between the period of the Rabi oscillation and the period of the Ramsey fringes, we obtain the Ramsey trajectories denoted by the evolution of $(z(t_2), \phi(t_2))$ in the phase space [see Figs. 5(a′) and 5(b′)]. As a result, we find that the phase-space areas enclosed by the two typical closed orbits (the Ramsey trajectory and the Rabi orbit) are identical.

It is worth emphasizing that the cavity field not only can play with the atoms interactively and modify their dynamics effectively, but also can carry with it information on the atomic population imbalance as it leaks out of the cavity. In Figs. 5(a) and 5(b), we show the time evolution of the atomic population imbalance and the number of intra-cavity photons (which is proportional to the cavity output), with the latter calculated from the former by using Eq. (3). We see that, in our weak atom–cavity-field coupling case, i.e., $\tilde{A}_h = 0.0001$, the

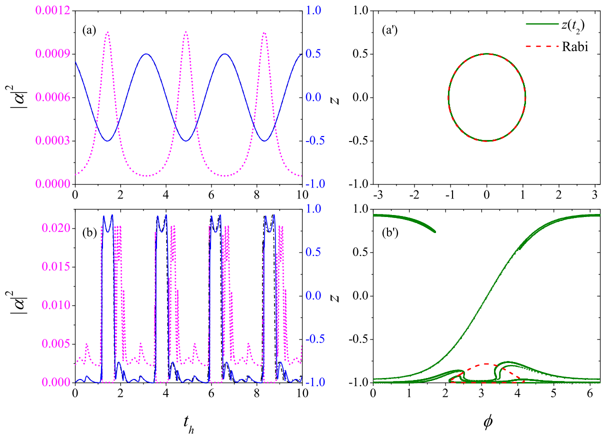

Fig. 5. Atomic population imbalance (blue solid lines) $z(t_2)$ and intra-cavity photon number (magenta dotted lines) $|\alpha(t_2)|^2$ versus the holding time t_h with $B = -0.8$ and $\tilde{A}_h = 0.0001$. The initial states are (a)[(a′)] $(z_0, \phi_0) = (-0.5, 0)$ and (b)[(b′)] $(z_0, \phi_0) \simeq (-1, 0)$. (a′) and (b′) demonstrate the Rabi orbits (red dashed lines) during the holding time t_h and the trajectories corresponding to Ramsey fringes (olive solid lines). The same parameters are used as in Fig. 2. The black dashed-dotted lines (almost overlapping with the blue solid lines) denote the case $\tilde{A}_h = 0$ for comparison.

Ramsey fringes recorded by the oscillation of the photon number can completely reflect the frequency information of the atomic interference, as demonstrated in Fig. 5(b). Moreover, two important properties are illustrated as well. (1) The holding-field-induced modification of the period (or the frequency) of the Ramsey fringes strongly depends on the initial state. For $z_0 = -0.5$, no modification is found, as shown in Fig. 5(a), while a small modification for $z_0 \simeq -1$ is seen in Fig. 5(b). (2) The amplitude of the Ramsey fringes characterized by the photon number can be largely enhanced by changing the initial atomic population imbalance between the two traps. Actually, when $z_0 \simeq B$, the maximum of the photon number will occur [see Eq. (3)]. For $B = -0.8$, the value of $|\alpha(t_2)|^2$ for $z_0 \simeq -1$ shown in Fig. 5(b) is more than 10 times that for $z_0 = -0.5$ displayed in Fig. 5(a). However, for the two different initial states, we find that the introduction of the weak atom-field coupling during the holding time cannot change the shape of the Ramsey fringes. Indeed, the fringes can encode the information on the atom-atom interaction [see Eq. (6)]. For the short pulses (e.g., $\omega > 10$), the period of the fringes monotonously increases with the atom-atom interaction when $r < 2.02$ and monotonously decreases with the atom-atom interaction when $r > 2.02$.

We have thoroughly investigated the nonlinear Ramsey interferometry in a coupled BJJ-cavity system and shown that both the atomic interaction and the cavity field play a significant role in the dynamical process. It is found that the Ramsey fringes are very sensitive to the initial state, and the frequency of the fringes can encode the information on both the atom-atom interaction and the atom–cavity-field coupling. In particular, for a weak holding field, it is found that the Ramsey fringes recorded by the oscillation of the photon number can completely reflect the frequency information of the atomic interference due to the weak atom–cavity-field coupling, which allows a nondestructive observation of the atomic Ramsey fringes via the transmission spectra of the cavity. For the system with more than two sites, the tunneling between different sites at least qualitatively causes a decay of the fringe visibility. This Letter may suggest the potential applications to both accurately calibrate the atomic parameters in trapped quantum gases and precisely manipulate the cold atoms in a full optical way.

Funding. National Natural Science Foundation of China (NSFC) (11547046, 11665020, 11547603, 11575027); China Postdoctoral Science Foundation (2015M580068); Natural Science Foundation of Gansu Province of China (1606RJZA081).

REFERENCES

1. N. F. Ramsey, Phys. Rev. **78**, 695 (1950).
2. J. Grond, U. Hohenester, I. Mazets, and J. Schmiedmayer, New J. Phys. **12**, 065036 (2010).
3. M. Egorov, B. Opanchuk, P. Drummond, B. V. Hall, P. Hannaford, and A. I. Sidorov, Phys. Rev. A **87**, 053614 (2013).
4. A. A. Wood, L. M. Bennie, A. Duong, M. Jasperse, L. D. Turner, and R. P. Anderson, Phys. Rev. A **92**, 053604 (2015).
5. S. Boixo, A. Datta, M. J. Davis, S. T. Flammia, A. Shaji, and C. M. Caves, Phys. Rev. Lett. **101**, 040403 (2008).
6. A. B. Tacla, S. Boixo, A. Datta, A. Shaji, and C. M. Caves, Phys. Rev. A **82**, 053636 (2010).
7. A. Smerzi, S. Fantoni, S. Giovanazzi, and S. R. Shenoy, Phys. Rev. Lett. **79**, 4950 (1997).
8. B. D. Josephson, Phys. Lett. **1**, 251 (1962).
9. F. Brennecke, R. Mottl, K. Baumann, R. Landig, T. Donner, and T. Esslinger, Proc. Natl. Acad. Sci. USA **110**, 11763 (2013).
10. Y. Ashida and M. Ueda, Phys. Rev. Lett. **115**, 095301 (2015).
11. J. Klinder, H. Keßler, M. Wolke, L. Mathey, and A. Hemmerich, Proc. Natl. Acad. Sci. USA **112**, 3290 (2015).
12. R. Landig, L. Hruby, N. Dogra, M. Landini, R. Mottl, T. Donner, and T. Esslinger, Nature **532**, 476 (2016).
13. N. Brahms, T. P. Purdy, D. W. C. Brooks, T. Botter, and D. M. Stamper-Kurn, Nat. Phys. **7**, 604 (2011).
14. W. Chen, J. Hu, Y. Duan, B. Braverman, H. Zhang, and V. Vuletić, Phys. Rev. Lett. **115**, 250502 (2015).
15. Y. Colombe, T. Steinmetz, G. Dubois, F. Linke, D. Hunger, and J. Reichel, Nature **450**, 272 (2007).
16. C. Zhu, L. Dong, and H. Pu, Phys. Rev. A **94**, 053621 (2016).
17. M. Reza Bakhtiari, A. Hemmerich, H. Ritsch, and M. Thorwart, Phys. Rev. Lett. **114**, 123601 (2015).
18. Z. Wang, J. Lian, J. Q. Liang, Y. Yu, and W. M. Liu, Phys. Rev. A **93**, 033630 (2016).
19. G. Szirmai, G. Mazzarella, and L. Salasnich, Phys. Rev. A **91**, 023601 (2015).
20. J. Huang, P. Gong, X. Qin, H. Zhong, and C. Lee, Phys. Rev. A **94**, 023618 (2016).
21. F. Haas, J. Volz, R. Gehr, J. Reichel, and J. Estève, Science **344**, 180 (2014).
22. R. McConnell, H. Zhang, J. Hu, S. Ćuk, and V. Vuletić, Nature **519**, 439 (2015).
23. P. Hamilton, M. Jaffe, J. M. Brown, L. Maisenbacher, B. Estey, and H. Müller, Phys. Rev. Lett. **114**, 100405 (2015).
24. H. Ritsch, P. Domokos, F. Brennecke, and T. Esslinger, Rev. Mod. Phys. **85**, 553 (2013).
25. B. Padhi and S. Ghosh, Phys. Rev. Lett. **111**, 043603 (2013).
26. J. M. Zhang, W. M. Liu, and D. L. Zhou, Phys. Rev. A **78**, 043618 (2008).
27. G. J. Milburn, J. Corney, E. M. Wright, and D. F. Walls, Phys. Rev. A **55**, 4318 (1997).
28. J. M. Zhang, W. M. Liu, and D. L. Zhou, Phys. Rev. A **77**, 033620 (2008).
29. P. Horak, S. M. Barnett, and H. Ritsch, Phys. Rev. A **61**, 033609 (2000).
30. A. J. Leggett, Rev. Mod. Phys. **73**, 307 (2001).
31. T. Köhler, K. Góral, and P. S. Julienne, Rev. Mod. Phys. **78**, 1311 (2006).